Cancer Immunol Immunother (2013) 62:1187–1197
DOI 10.1007/s00262-013-1423-9

ORIGINAL ARTICLE

Therapy model for advanced intracerebral B16 mouse melanoma using radiation therapy combined with immunotherapy

Henry M. Smilowitz · Daniel Sasso · Edward W. Lee · Gyuhyeong Goh · Peggy L. Micca · F. Avraham Dilmanian

Received: 28 December 2012 / Accepted: 30 March 2013 / Published online: 25 April 2013

Abstract A reproducible therapy model for advanced intracerebral B16 melanoma is reported. Implanted tumors (D0), suppressed by a single 15 Gy radiosurgical dose of 100 kVp X-rays (D8), were further suppressed by a single ip injection of a Treg-depleting mAb given 2 days prior to the initiation (D9) of four weekly then eight bi-monthly sc injections of GMCSF-transfected, mitotically disabled B16 cells. The trends of seven independent experiments were similar to the combined result: The median (days) [SD/total *N*] of survival went from 15[1.09/62] (no treatment control) to 35.8[8.8/58] (radiation therapy only) to 52.5[13.5/57] (radiation therapy plus immunotherapy). Within 2 weeks after immunization, tumors in mice receiving radiation therapy plus immunotherapy were significantly smaller than tumors in mice treated only with radiosurgery. Splenocytes and lymph node cells from immunized mice showed increased interferon γ production when cultured with syngeneic tumor cells. We suggest that our model will be useful for the development and testing of novel combination therapies for brain tumors.

H. M. Smilowitz (✉) · D. Sasso · E. W. Lee
Department of Cell Biology, University of Connecticut Health Center, 263 Farmington Avenue, Farmington, CT 06030, USA
e-mail: smilowitz@nso1.uchc.edu

G. Goh
Department of Statistics, University of Connecticut, 215 Glenbrook Road, Storrs, CT 06269-4120, USA

P. L. Micca
Medical Department, Brookhaven National Laboratory, Upton, NY 11973, USA

F. A. Dilmanian
Department of Radiation Oncology and Neurology, State University of New York, Stony Brook, NY 11794-7028, USA

Keywords B16 melanoma · Mouse · Brain tumor · Radiation therapy · Immunotherapy

Background

It is estimated that there are ~200,000 brain tumor cases in the United States each year of which most (~160,000) are brain metastases [1, 2]. The median survival of these patients after diagnosis is currently measured in months [3]. Clearly, improvements in therapy are urgently needed to address brain metastases.

While melanomas represent 3–5 % of primary solid tumors [4], ~20 % of those patients develop metastases that have a very high likelihood (~40–75 %) of involving the brain [4]. Hence, for therapy regimens of metastatic disease to be widely durable, they must be capable of treating brain metastases too. There has been increasing interest in the use of immunotherapy for cancer in general and metastatic melanoma in particular [5]. A review of 56 Phase II and III clinical trials of vaccine therapy for 4375 stage IV melanoma patients revealed that ~25 % of the study population experienced some benefit from a form of immunotherapy but no overall survival benefit over other therapies [6]. More recently, ipilimumab has shown to prolong overall survival by 4 months [7] with efficacy for some patients with brain metastases [8]. Adoptive immunotherapy using engineered T cells recently has been reported to have significant efficacy for both systemic and intracerebral melanomas [9], but logistical hurdles will need to be overcome before such strategies can become widely available. Hence, there is still great interest in developing cost-effective strategies for active immunotherapy of melanoma [10] including combination therapies [11]. Our strategy is to identify clinically translatable

regimens that are very effective in rigorous, clinically relevant animal models, and then to test the most successful of these in clinical trials. Toward that end, we have developed an advanced intracerebral melanoma therapy model in the mouse using the B16 melanoma [12]. Our model differs from most of the other experimental brain tumor models studied in that brain tumor therapy in our study is initiated when the tumors are well formed, vascularized, and advanced, that is, ~50–60 % of the time between tumor cell implantation and the time the mouse is required to be euthanized (virtual death). This model is now being used to devise and rigorously test combination therapies for intracerebral melanoma.

Materials and methods

Cell culture

B16 cells obtained from the ATCC (Manassas, VA) and PancO2 murine pancreatic adenocarcinoma [13] obtained form the NCI tumor bank (Frederick, MD) were grown on Sarstedt tissue culture Flasks (Newton, NC) in DMEM-CM (GIBCO #11995) supplemented with glutamine (2 mM), Penn/Strep (100 U/ml penicillin; 100 μg/ml streptomycin), and Fungizone (0.25 μg/ml) all from Invitrogen (Grand Island, NY).

In vivo experimentation

All of the work and study protocols performed were approved by the University of Connecticut Health Center Animal Care and Use Committee.

Mouse anesthesia

Briefly, C57/BL6 mice (Charles River), each weighing approximately 18–20 g, were anesthetized by intraperitoneally injecting approximately 0.06 ml/20 g of a Ketamine/Xylazine mixture containing 1.1 ml phosphate buffered saline, 1.0 ml Ketamine solution (20 mg/ml, Lederle Parenterals, Inc.), and 0.11 ml xylazine solution (20 mg/ml, Ben Venue Labs).

Intracerebral tumors

Intracerebral B16 melanoma tumors were initiated by injecting 200 cultured untreated cells mixed together with 1,800 disabled cells [pre-irradiated by 100 Gy (several hours before implantation) in a volume of 1.0 μl into the brains of C57BL6 mice (Charles River, Kingston, NY)], isogeneic with the B16 tumor. Briefly, tumors were initiated in deeply anesthetized mice by inoculating 1 μl of culture medium containing the tumor cells into the left striatum ~3 mm deep at a point along the (serrated) coronal suture approximately halfway between the mid-sagittal line and the cranial insertion of the left temporalis muscle (~5 mm posterior to the interocular plane). At that point, a 0.5-mm burr hole was drilled through the skull, and a 27-gauge needle (fitted with a depth-limiting plastic collar to ensure cell injection ~3 mm beneath the skull) that was connected to a 1-μl Hamilton microsyringe by flexible tubing was then inserted into the burr hole. Following a steady 30-s infusion of the cells, another 30 s was allowed for the cells to settle before withdrawing the inoculation needle from the brain. This technique [13] resulted in a locally expanding and partially infiltrating tumor of the striatum and around the needle track, with no evidence of blood- or cerebrospinal fluid-borne metastases. Untreated, mice had to be euthanized 13–20-day post-implantation (median ~day 15.5) when the mice showed signs of imminent death from a large intracerebral melanoma.

Irradiations

Irradiations were performed at the Philips RT100 X-ray facility located at Brookhaven National Laboratory (Upton, NY) 8 days after tumor implantation. The beam was filtered with 1.7 mm Al. A 3.5-mm-thick, 30.7-mm-high, 30.5-mm-wide lead shield containing a 6-mm-wide, ~9.5-mm-high rectangular notch was taped to one vertical side of a movable plastic block (Fig. 2A). Each anesthetized mouse was positioned prone on the flat horizontal surface of the block, and its left foreleg drooped over the edge of the block, apposed to the caudal edge of the lead shield. The mid-interocular line of the anesthetized mouse was made horizontal by rotating its head by its ears manually, and the mid-sagittal plane of the head was swiveled manually ~12° from the sagittal to allow the irradiated zone of the head to be as close to the RT-100's anodal focal point as was mechanically and anatomically feasible for the individual mouse. In this manner, the anteroinferior corner of the notch was noted to be about 0–2 mm below the posterior canthus of the left palpebral fissure—that dimension varying according to the size of the individual mouse's head. After the mouse was so positioned, the site of tumor initiation was near the middle of the 6-mm-wide rectangular notch in the shield, and the block was slid and swiveled on its supporting table to expose the notch symmetrically to the vertical, circular, 25 mm diameter open end of the RT-100's irradiation gun, the mouse's anteroposterior axis pointing in the direction of the RT-100's electron beam.

Dosimetry

The BNL Medical Department Phillips RT-100 was operated at 100 kVp, 8 mA, and the beam was filtered with

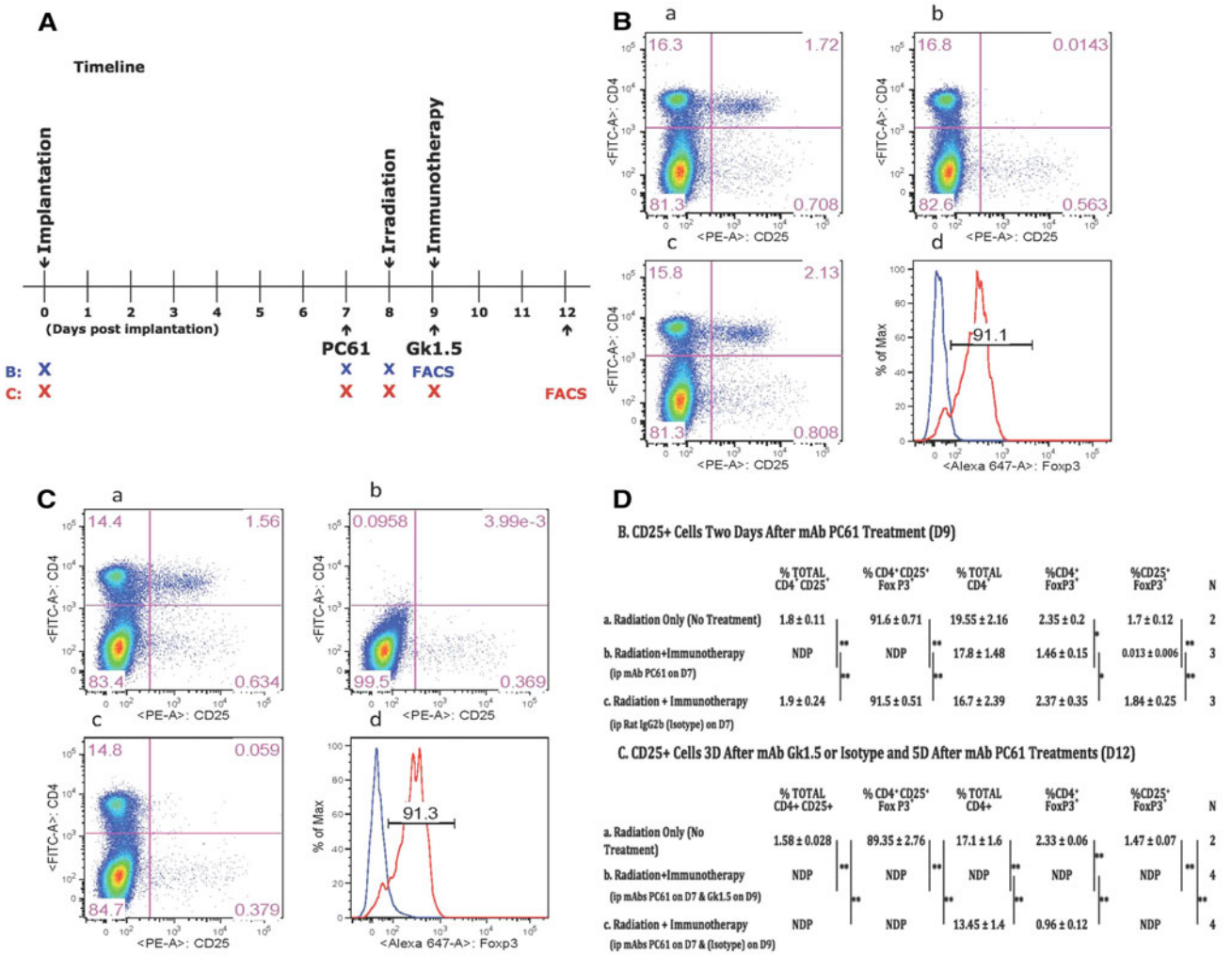

Fig. 1 Depletion of CD4+CD25+ cells by PC61 and of CD4+ cells by Gk1.5. **A** Timeline of manipulations. *Upward arrow*, day (D) of treatment; *cross symbol*, treatment. **B** *a* Radiation only (R) mice (no other treatment); *b* radiation+immunotherapy (R+I) mice received PC61, D7; *c*, R+I mice received Rat IgG2b, D7; *d* FoxP3 and isotype control (performed on all samples). **C** Depletion of CD4 cells assayed D12: *a* radiation only (R) mice (no other treatment); *b* radiation+immunotherapy (R+I) mice received PC61, D7 and Gk1.5, D9; *c* R+I mice received PC61, D7 and Rat IgG2b, D9; *d* FoxP3 and isotype control (performed on all samples). **D** Summary table: mean ± SD, *N* and statistical significance (**$p < 0.01$; *$p < 0.05$). *NDP* no detectable population (100,000 cells collected)

1.7 mm Al, resulting in a median beam energy of 37 keV. The source-to-aperture distance was 10 cm. The 3.5-mm-thick shield effectively blocked beam penetration. The dose rate 3 mm deep in the brain, around the tumor's isocenter, was calculated to be a nominal 7.6 Gy/min using an absolute calibration of a radical ion chamber and its electrometer and 2 min measurements of the dose in the ion chamber and the electrometer prior to each session.

Immunotherapy

Seven days post-tumor implantation mice received an ip injection of 0.5 mg mAb PC61 directed to CD25, the alpha subunit of the IL-2 receptor [14] (National Cell Culture Center, Milwaukee, WI) to reduce the number of T regulatory cells (Tregs). Figure 1 shows that CD4+CD25+ cells (of which >90 % are FoxP3+) are reduced 99 % 2 days after PC61 injection. About ~50 % of CD4+FoxP3+ Treg cells are depleted by PC61 treatment (Fig. 1D), a value consistent with previous findings [15]. Nine days post-tumor cell implantation mice received the first subcutaneous (sc) injection of 10^6 irradiated (100 Gy) granulocyte macrophage colony stimulating factor (GMCSF)-transfected B16 cells (B16-GMCSF) (kindly provided by Glenn Dranoff, Harvard Medical School, Boston, MA) [16] which was repeated weekly (four total) and then bimonthly (up to 4 months).

CD4 cell depletion study

Starting 9-day post-tumor cell implantation, ten mice in the radiation therapy plus immunotherapy group received their first ip injection of 200 μg rat anti-mouse CD4 (Gk1.5, BioXCell, W. Lebanon, NH). Injections were repeated every 3 days for a total of eight injections (3 weeks). Figure 1B shows that CD4+ cells are reduced >99 % 3 days after the first Gk1.5 injection. Immunotherapy was as described above.

ELISPOT assay

The enzyme-linked immunospot (ELISPOT) assay was used to quantify cells secreting interferon gamma (IFNγ) as spots on 96-well plates. An ELISPOT kit was used (BD Biosciences Cat # 551083) according to manufacturer's instructions. Splenocytes and cells from the subiliac lymph node draining the immunization site were prepared from naïve control mice (C), B16-implanted mice that received radiation therapy only (R) or radiation plus immunotherapy (R+I). Briefly, cells recovered from crushes of crudely minced tissues were filtered (40 μm strainer) and centrifuged. Erythrocytes were lysed by resuspension of pellets in 2 ml TAC buffer (13.1 mM Tris pH 7.2; 139.6 mM ammonium chloride) for 5 min followed by 10 ml cell culture medium and centrifuged again. Splenocytes and lymph node cells were resuspended in 5 and 2.5 ml cell culture medium, respectively, and counted. Splenocytes or lymph node cells (100,000) and 40,000 tumor cells (B16 or PANCO2) were added per well. Negative controls (no tumor cells) and positive controls [5 ng/ml PMA (Phorbol 12-myristate 13-acetate) and 500 ng/ml Ionomycin (PMA/I)] were used. Each condition was plated in duplicate and averaged. A dissecting stereo-microscope with attached digital camera was used to photograph each well. Image-J software was used to quantify the area subsumed by the spots using Image-J's intelligent background subtraction, auto threshold, and particle analysis functions.

Quantification of intracerebral B16F10 tumors using in vivo luciferase bioluminescence

Approximately 250 B16F10-LUC2 cells (PerkinElmer) were mixed with 5,000 irradiated (~100 Gy) B16 cells and implanted in the brains of C57Bl6 mice. After 7 days, the brains of the mice were imaged using an IVIS Spectrum In Vivo Imaging System (Caliper Life Sciences, Hopkinton, MA). Briefly, mice were anesthetized with 2 % isoflurane plus oxygen, shaved, and imaged for 120, 60, 30, 15, 5, and 1 s, 13 min following a sc injection of 75 mg/kg D-Luciferin (Caliper Life Sciences, Hopkinton, MA.). Photons per minute were obtained after selecting a region of interest that encompassed the portion of the head containing the tumor.

FACS analysis of antibody depletions

Eighteen mice implanted intracerebrally with B16 melanoma cells were irradiated on day 8 after implantation (D8). Four mice received no further treatment (radiation only). Of the 14 irradiated mice, 11 mice received a single injection of 0.5 mg mAb PC61 (anti CD25) on D7 and of these, 4 also received a single injection of 0.2 mg mAb Gk1.5 (anti CD4) on D9, and 4 received a single injection of 0.2 mg of Rat IgG2b (Gk1.5 isotype) on D9. Three mice received 0.5 mg of the rat IgG2b (PC61 isotype) on D7 (Fig. 1A). On day 9, after tumor cell implantation, two radiation only, three PC61 (D7) and three isotype (D7) mice were euthanized, and cell suspensions prepared from their spleens were labeled as indicated (Fig. 1B, D). On D12, two radiation only, four PC61+Gk1.5 and four PC61+RatIgG2b were euthanized, and cell suspensions prepared from their spleens and labeled as indicated (Fig. 1C, D). 1B: FITC-αmCD4 (FITC rIgG2b), PE-αmCD25 (PErIgG1), AF647-αmFoxP3(AF647rIgG2b). 1C: APC-αmCD4(APCrIgG2b), PerCP-αmCD8(PerCPrIgG2a), FITC-αmCD3(FITCrIgG2b).

Interpretation of data: survival curves

The Wilcoxon log-rank test was used to compare median survival among the treatment groups. Some animals lived a year and were right censored at 365 days. Statistical evaluation of results was in two steps. First, for each experiment, we compared R and R+I groups and used the unadjusted p value from the log-rank test and alpha level of significance of 0.05. Second, we compared C versus R and C versus R+I groups and report Bonferroni corrected p values to account for the two additional tests being conducted. Analyses were conducted using the LIFETEST procedure in SAS. *Tumor size*—Wilcoxon nonparametric rank sum analysis—appropriate for small groups of animals was used to assess the likelihood that the size of the tumors in two groups of mice was the same or different. *ELISPOT assay*—These data were analyzed using a two-factor ANOVA with the factors treatment (c, r, r+i) and challenge (no, b16, panc02, and pma) and the two-factor interaction term. p values for subgroup comparisons were estimated using the LSMEANS option in the GLM procedure in SAS. *Depletion assay*—For the antibody depletion data, we used a one-way ANOVA, followed by Tukey's HSD test, to compare the group means [a, R (no treatment) versus b, R+I (depleting antibody treatment) versus c, R+I (isotype antibody treatment) for A, (PC61) and B, (Gk1.5) antibodies at the $\alpha = 0.01$ or 0.05 levels (**, *)], respectively.

Results

Combination of radiation therapy and immunotherapy for advanced intracerebral melanoma

To study the efficacy of the combination of radiation therapy and immunotherapy for advanced intracerebral (ic) melanomas, mice implanted ic with B16 melanoma on D0 received either no treatment (C), radiation only (R) on D8 when the tumors were advanced or radiation+immunotherapy (R+I) (see "Materials and methods"). Figure 2a shows the positioning of mice prior to irradiation. Each exposure lasted 2 min corresponding to an average tumor dose of 15 Gy. This dose is well tolerated; mice live without any signs of illness or weight loss for at least a year. Figure 2b shows a typical swath of non-pigmented fur that develops at the site of irradiation after ~2–4 months after irradiation. Table 1 summarizes the data of the seven independent experiments that were performed and the aggregate data of all seven experiments combined. In five of the seven independent experiments (A, B, D, E, F), the comparison of R to R+I was statistically significant. However, the aggregate of all seven experiments was highly statistically significant. All of the comparisons of C versus R+I were statistically significant as was the aggregate. In three of the seven independent experiments, the comparison of C and R was statistically significant as was the aggregate. All of the comparisons of the aggregate of the seven experiments were highly statistically significant ($p < 0.0001$). Figure 2a, b shows the Kaplan–Meier survival plots of mice that correspond to experiments F and A in Table 1, respectively. Table 1 also summarizes the seven experiments in aggregate, the median day of virtual death for untreated, radiation-only and radiation plus immunotherapy groups ±SD was 15 ± 1.09, 35.8 ± 8.8, and 52.5 ± 13.5, respectively. Figure 2c shows the aggregate Kaplan–Meier survival plot of the seven separate experiments summarized in Table 1. The Wilcoxon log-rank test was used to compare median survival among the treatment groups of each of the seven experiments and the aggregate of all seven experiments. It can be seen that the p value of the comparison between radiation therapy only and radiation therapy plus immunotherapy was <0.05 in five of the seven individual experiments. The p value of all comparisons in the aggregate analysis (Fig. 2c) was <0.0001. Hence, survival of mice with advanced intracerebral melanoma that received radiation plus immunotherapy is greater than mice with similar tumors that received either no treatment or 15 Gy radiation therapy only. Further, survival of mice with advanced intracerebral melanoma that received 15 Gy radiation therapy only is greater than mice with similar tumors that received no treatment.

Tumors in mice with advanced intracerebral melanoma that received radiation plus immunotherapy are smaller than those found in radiation-only-treated mice

Seven days after the implantation of 250 B16F10 luciferase expressing cells (B16F10-LUC2) into the brains of twenty-six C57BL6 mice, the size of each of the tumors was determined using the IVIS (see "Materials and methods"), and the mice were split into two groups with roughly equivalently sized tumors in each group (Group A median tumor size = 970,000 counts/min and mean tumor size = 1,983,000; Group B median tumor size = 1,025,000 counts/min and mean tumor size = 1,902,150). The R+I group (B) received 0.5 mg PC61 on day seven. On the eighth day, both R (A) and R+I (B) groups received radiation therapy (15 Gy) (see "Materials and methods"). On the ninth day, the mice in the R+I group (B) also received their first immunotherapy treatment that was repeated on day 16 (see "Materials and methods"). Imaging was then performed 22 days after tumor cell implantation (13 days after radiation therapy). Figure 3 is a plot of the ratios of the sizes of intracerebral melanomas (photons/min) in the two groups (see "Materials and methods") on D21/D7. The median ratio Group A = 0.885 whereas the median ratio Group B = 0.28. Wilcoxon nonparametric statistics indicates that the two groups A and B differ from one another ($p < 0.02$).

Splenocytes and lymph node cells from mice treated with radiation plus immunotherapy have increased numbers of cells that produce interferon γ when cultured either with tumor cells syngeneic for C57Bl/6 mice or non-specifically activated with PMA/Ionomycin as revealed by the ELISPOT assay

Splenocytes and cells from the subiliac lymph node draining the immunization site, isolated (see "Materials and methods") from naïve control mice (c), mice treated for intracerebral melanoma by radiation therapy only (r) and mice treated for intracerebral melanoma by radiation plus immunotherapy (r+i) were added to wells of ELISPOT dishes at 100,000 cells/well (see "Materials and methods") with either no additions, B16 cells (40,000), PANC-02 cells (40,000), or 5 ng/ml PMA/500 ng/ml Ionomycin and cultured for 18 h. Spots representing IFNγ production were revealed and quantified according to section "Materials and methods." The data obtained using surviving mice 1, 2, and 3 weeks after the initiation of immunotherapy were pooled as were data from surviving mice 4–7-week post-initiation of immunotherapy. Figure 4 shows that splenocytes from r+i-treated mice 1–3 weeks after the start of immunotherapy when incubated with

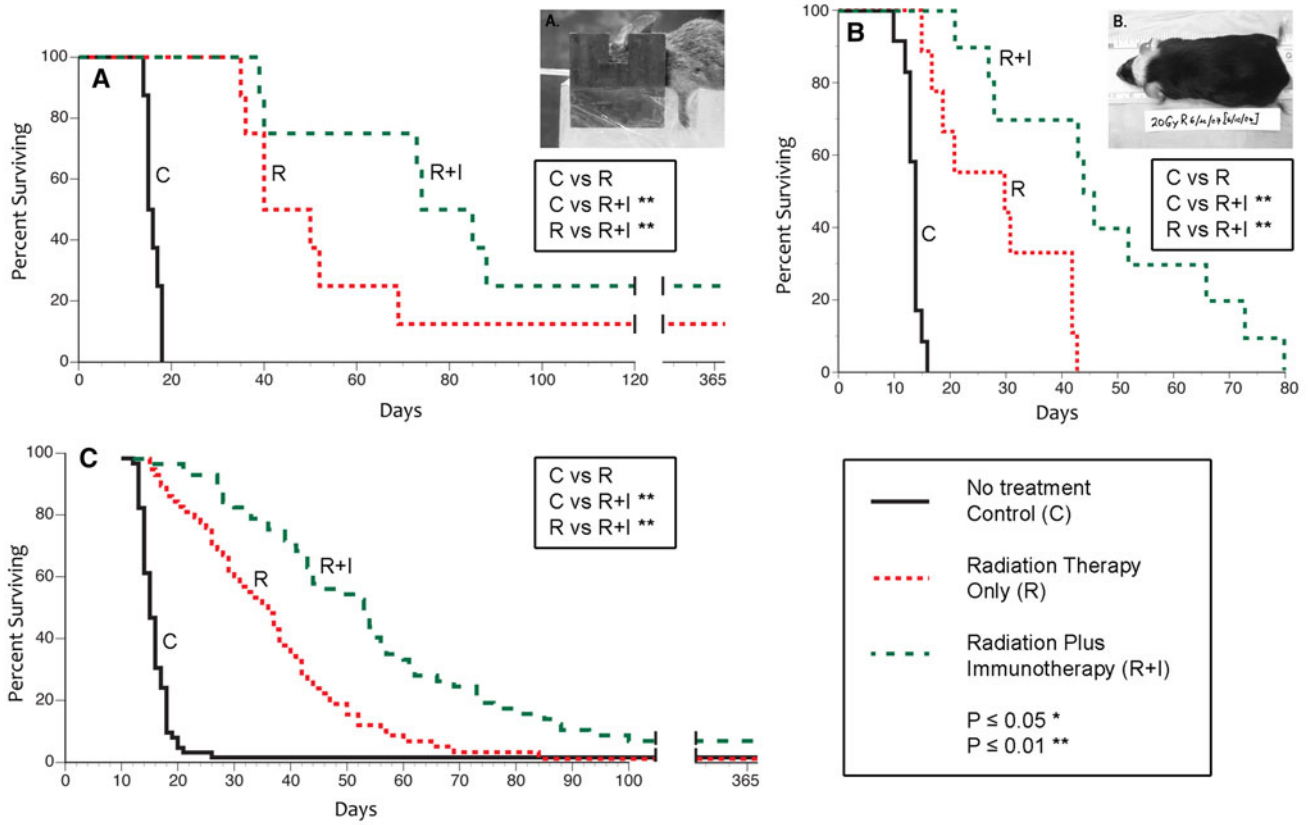

Fig. 2 The combination of radiosurgery and immunotherapy for advanced intracerebral B16 melanoma in mice. Mice bearing advanced intracerebreal B16 tumors were irradiated as described in section "Materials and methods" 8-day post-implantation. **A** shows a mouse positioned for irradiation as described in "Materials and methods." **B** shows a mouse with a swath of non-pigmented fur that develops at the site of irradiation after 2–4 months. **A**, **B** shows two of the seven independent experiments that were performed and summarized in Table 1. **C** shows all seven experiments summarized in Table 1 combined. Wilcoxon log-rank tests were used to compare median survival among groups (see Table 1 for p values and "Materials and methods" for details)

PANCO2 cells or PMA/I produce statistically greater IFNγ ($p < 0.05$) than splenocytes from c or r mice when incubated with PANC02 or PMA/I. This result is true for lymph node cells isolated from r+i-treated mice 4–7 weeks after the start of immunotherapy. Incubation of cells from spleens of immunized mice (1–3 weeks) with B16 cells showed increased levels of IFNγ that showed the same trend but was not statistically different ($p < 0.09$). For lymph node cells and splenocytes isolated 1–3 and 4–7 weeks, respectively, after the initiation of immunotherapy, only incubation with PMA/I resulted in statistically greater IFNγ production ($p < 0.05$) than the corresponding cells from c or r mice. The data support the hypothesis that splenocytes and cells from lymph nodes draining the site of immunization from mice treated with radiation and immunotherapy are immune primed compared with cells from control mice and mice receiving radiation therapy only and such cells produce increased levels of IFNγ when either stimulated with PMA/I or when incubated with some tumor cells syngeneic to the host.

Abrogation of immunotherapy-induced life extension by anti-CD4 antibody treatment

To test the hypothesis that CD4 T cells play a role in the immunotherapy-induced life extension we obtain, one group of ten mice receiving radiation therapy plus immunotherapy also received eight ip injections of anti-CD4 mAb Gk1.5 (200 μg/mouse) every 3 days starting on day 9 (the first day of immunotherapy). Figure 5 shows that the untreated control group differs from radiation-only-treated mice ($p < 0.003$) and from radiation plus immunotherapy-treated mice ($p < 0.0001$). Further, radiation-only-treated mice differ from mice receiving radiation plus immunotherapy ($p < 0.04$). However, radiation-only and radiation plus immunotherapy-treated mice did not differ from radiation plus immunotherapy mice additionally treated with anti-CD4 mAb ($p < 0.99$, $p < 0.52$, respectively). These data support the hypothesis that mice receiving radiation therapy plus immunotherapy mount a T cell response to the intracerebral B16 tumor that has a component of CD4 T cell dependency.

Table 1 Combination of radiation therapy and immunotherapy for advanced intracerebral B16 melanoma in mice

	Untreated control (C)	Radiation therapy only (R)	Radiation therapy+immuno therapy (R+I)	*p* values		
				R versus R+I	R versus C	R+I versus R
A	14 (10–16)	30 (15–43)	45 (21–80)	0.005**	0.015*	<0.0001**
	$N = 12$	$N = 9$	$N = 10$			
B	16 (13–#)	28.5 (24–60)	53 (28–100)	0.004**	0.18	0.0003**
	$N = 14$	$N = 10$	$N = 11$			
C	15 (13–18)	36.5 (18–56)	42.5 (12–#)	0.3	0.02*	0.0003**
	$N = 10$	$N = 10$	$N = 10$			
D	17 (13–21)	23 (13–29)	43.5 (39–60)	0.005**	0.99	0.0011**
	$N = 5$	$N = 5$	$N = 4$			
E	15 (13–16)	50 (37–84)	72 (56–93)	0.05*	0.23	0.0002**
	$N = 5$	$N = 5$	$N = 4$			
F	17.3 (14–26)	38 (16–57)	54 (21–#)	0.04*	0.22	<0.0001**
	$N = 8$	$N = 11$	$N = 10$			
G	15.5 (14–18)	45 (35–#)	79.5 (39–#)	0.28	0.01*	<0.0001**
	$N = 8$	$N = 8$	$N = 8$			
A–G	15 (10–26)	35.8 (13–#)	52.5 (12–#)	<0.0001**	<0.0001**	<0.0001**
	$N = 62$	$N = 58$	$N = 57$			

Seven independent experiments were performed as described in "Materials and methods." Shown are the median survival in days, the range in parentheses, and the number of Mice (*N*) in each group. Wilcoxon log-rank tests were used to compare median survival among groups (see "Materials and methods" for details)

Mice that lived for a year

* $p \leq 0.05$; ** $p \leq 0.01$ II versus I and III versus I, Bonferroni corrected *p* values

Discussion

We have developed a therapy model for advanced intracerebral melanoma that utilizes the extremely aggressive and widely used B16 melanoma model. Therapy consists of a single dose of sub-optimal radiation therapy (15 Gy X-rays delivered via a Philips RT-100 irradiator) and immunotherapy [in this case a single dose of mAb PC61 to reduce Tregs followed by multiple doses of irradiated and clonogenically disabled GMCSF-secreting B16F10 cells (GVAX)]. X-ray therapy is not started until day 8 after B16 cell implantation—a time when the tumor is more than half way between the time of implantation and the time of death (median, D15.5). Melanoma brain metastases have been modeled since the mid-1970s using the subcutaneous, intravenous, intracarotid, intracardiac, and intracerebral tumor initiation routes [reviewed, 17]. Each approach offers advantages and disadvantages when used for therapy studies [17, Table 3, 18]. Our intracerebral implantation model is unique as it combines external radiation therapy and immunotherapy to treat advanced intracerebral tumors. The use of a rigorous model at an advanced stage of tumor development addresses key problems that may be inherently associated with preclinical mouse models as useful predictors of therapy regimens effective in humans [19, 20]. The model can be made more rigorous by starting therapy later and/or by irradiating less. Long-term survival is at ~10 %, suggesting that additional regimens that provide further benefit should be observable. Hence, we are using this model to develop and compare clinically relevant combinatorial therapies.

The use of external-beam radiation therapy to debulk advanced intracranial tumors in combination with immunotherapy has been studied to a greater extent for gliomas [21] than for melanomas. Previously, a study combining boron neutron capture therapy with immunotherapy for advanced 9L gliosarcomas occupying 2 % of the rat brain at the time of therapy initiation was one of the first of such studies for advanced tumors [22, 23]. Since then, radiation therapy has been combined with immunotherapy and other combination strategies to treat experimental gliomas and other tumors [21, 24]. The combination of radiation therapy, chemotherapy, and immunotherapy for glioma is currently being tested in clinical trials [25, 26]. We suggest that our preclinical model of advanced intracerebral melanoma can be used to test a large number of combination therapies relatively inexpensively—the most successful of which could then be translated to

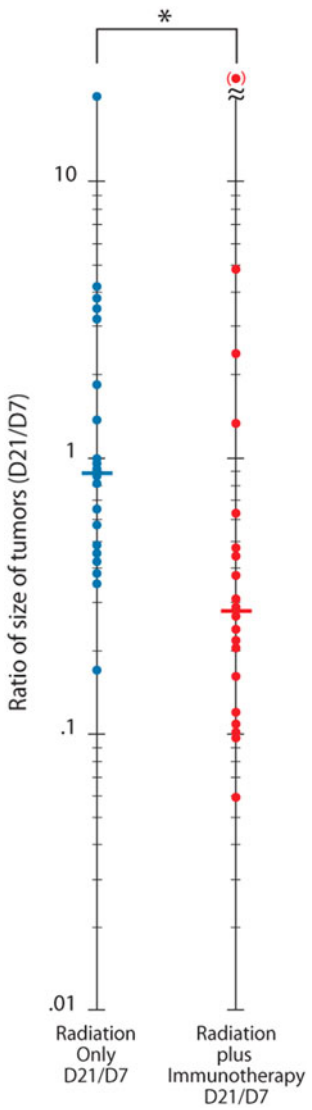

Fig. 3 Tumors in mice with advanced intracerebral melanoma that received radiation plus immunotherapy are smaller than those found in radiation-only-treated mice. Seven days after the intracerebral implantation of 250 luciferase expressing B16F10 cells (B16F10-Luc2), bioluminescence was quantified and mice were sorted into two groups with similar distributions of tumor sizes. All mice were irradiated (15 Gy) ("Materials and methods"). In addition, half the mice received immunotherapy and received the first vaccination on day 9 ("Materials and methods"). The ratios of tumor size (counts/min) on day 21 divided by tumor size on day 7 is shown for radiation-only and radiation plus immunotherapy groups. *Circle* each mouse, *Parentheses circle* dead mouse

clinical trials for the treatment of melanoma that has spread to the brain [27].

We have confirmed that 99 % of CD4+CD25+ cells (of which ~90 % are FoxP3+) were depleted 2 days after the injection of 0.5 mg mAb PC61 (Fig. 1B) while CD4+FoxP3 Treg cells are depleted about 50 % (Fig. 1D, Table). It has been shown that under such conditions CD4+CD25+ cells and CD4+FoxP3+ cells return with time [15, 28]. Such partial and transient depletions of Treg cells have been shown to increase the generation and function of tumor-specific CD8 T cells in response to vaccination in a variety of tumor models that resulted in enhanced immunotherapy and prolongation of life [29–33, to cite a few]. For this reason, an initial depletion of CD4+CD25+ cells prior to the first immunization was incorporated into our protocol.

GM-CSF secreting autologous tumor cell vaccine is effective at inducing an immune response in intracerebral tumor bearing and irradiated isogeneic mice. The GMCSF secreted in vivo by the transfected cells can be expected to increase the population of migratory dendritic cells (DC) and DC in lymphoid tissue and promote the induction of Th1-type immune responses after vaccination, which are important to the anti-tumor response [34].

Our data show that virtually all of CD4+ cells are depleted 3 days after the first injection of anti-CD4 mAb on day 9, the day of the first immunization. Since the mice received a similar injection of anti-CD4 mAb every 3 days for 3 weeks, CD4 T cells should have remained depleted to some degree from 9- to 30-days post-tumor cell implantation. It is reported that CD4 T cells return slowly (~20 % after the first month, ~40 % after the second month, and ~100 % after 100 days) after depletion [35]. Therefore, any residual immunotherapy efficacy observed could be due to the return of CD4 cells and/or the contribution of CD8 T cells. Depletion of both CD4 and CD8 T cells might be expected to inhibit the effects of immunotherapy more completely.

As has been the general experience with tumor vaccines, the anti-tumor response is not durable. A variety of mechanisms are now known that serve to limit the sustainability of active immunotherapy against cancer. For example, GM-CSF has also been shown to augment the proliferation and function of Tregs that may serve to limit the efficacy of GM-CSF secreting cell vaccines [36]. This may be part of the explanation as to why long-term survival is so low in this immunotherapy model. Therefore, additional strategies to decrease Tregs [37, 38]—such as the use of low-dose cyclophosphamide [39] and/or the checkpoint blockade inhibitor mAb, anti-CTLA-4 [40]—can now be tested in this system. Other clinically relevant combinatorial strategies to alter the immunosuppressive tumor environment, utilize immunotherapy-compatible chemotherapy, improve immunization schemes, enhance tumor debulking, and reduce T cell anergy/fatigue now can be tested and compared in our rigorous model. The most successful of these combinatorial strategies may be considered candidates for translation to clinical trials.

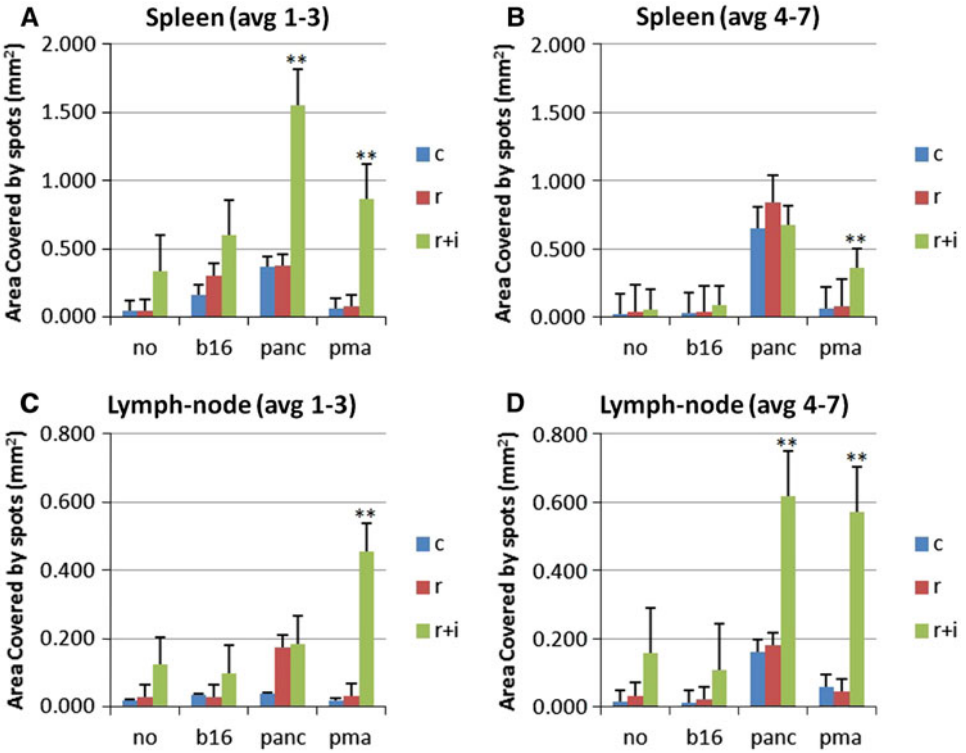

Fig. 4 ELISPOT assay: splenocytes and lymph node cells from mice treated with radiation plus immunotherapy have increased numbers of cells that produce IFNγ when cultured either with tumor cells syngeneic for C57Bl/6 mice or non-specifically activated with PMA/Ionomycin. Splenocytes and lymph node cells, prepared from control (naïve) mice and surviving mice whose intracerebral tumors were treated with radiation only and radiation plus immunotherapy, were added to microwells with no added cells, B16 or PANC02 cells or PMA/Ionomycin for 18 h prior to the development of spots for IFNγ ("Materials and methods"). Data from mice 1–3 and 4–7 weeks after the initiation of immunotherapy were pooled and shown in Fig. 3. Spleen (1–3): Panc and PMA: c versus r+i**, r versus r+i**, spleen (4–7): PMA: c versus r+i**, r versus r+i**, lymph node (1–3): PMA: c versus r+i**, r versus r+i**, lymph node: Panc and PMA: c versus r+i**, r versus r+i** (**$p \leq 0.01$)

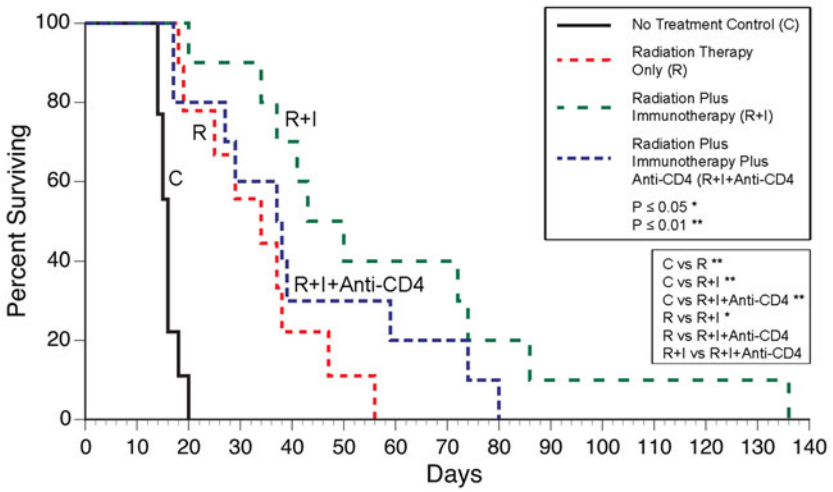

Fig. 5 Abrogation of immunotherapy-induced life extension by anti-CD4 antibody treatment. Mice were implanted intracerebrally with 200 B16 cells on day 0. No treatment control (C) radiation only (15 Gy, day 8) (R); radiation+immunotherapy (R+I); radiation+immunotherapy+anti-CD4 (eight ip injections of anti-CD4 mAb Gk1.5 (200 μg/mouse) every 3 days starting on day 9, the first day of immunotherapy) (R+I+anti-CD4). C differs from R ($p < 0.003$) and from R+I ($p < 0.0001$). Further, R differs from R+I ($p < 0.04$). However, R- and R+I-treated mice did not differ from R+I+anti-CD4 ($p < 0.99$; $p < 0.52$, respectively)

Acknowledgments We thank Dr. Daniel N. Slatkin for his advice and the technical support he provided for some of these experiments.

Conflict of interest The authors declare that they have no conflict of interest in any form with respect to this article.

References

1. Walbert T, Gilbert MR (2009) The role of chemotherapy in the treatment of patients with brain metastases from solid tumors. Int J Clin Oncol 14:299–306. doi:10.1007/s10147-009-0916-1
2. Langley RR, Fidler IJ (2013) The biology of brain metastasis. Clin Chem 59:180–189. doi:10.1373/clinchem.2012.193342
3. Goulart CR, Mattei TA, Ramina R (2011) Cerebral melanoma metastases: a critical review on diagnostic methods and therapeutic options. ISRN Surg 2011:276908. doi:10.5402/2011/276908
4. Preusser M, Capper D, Ilhan-Mutlu A, Berghoff AS, Birner P, Bartsch R, Marosi C, Zielinski C, Mehta MP, Winkler F, Wick W, von Deimling A (2012) Brain metastases: pathobiology and emerging targeted therapies. Acta Neuropathol 123:205–222. doi:10.1007/s00401-011-0933-9
5. Mellman I, Coukos G, Dranoff G (2011) Cancer immunotherapy comes of age. Nature 480:480–489. doi:10.1038/nature10673
6. Chi M, Dudek A (2011) Vaccine therapy for metastatic melanoma: systematic review and meta-analysis of clinical trials. Melanoma Res 21:165–174. doi:10.1097/CMR.0b013e328346554d
7. Hodi FS, O'Day SJ, McDermott DF, Weber RW, Sosman JA, Haanen JB, Gonzalez R, Robert C, Schadendorf D, Hassel JC, Akerley W, van den Eertwegh AJ, Lutzky J, Lorigan P, Vaubel JM, Linette GP, Hogg D, Ottensmeier CH, Lebbé C, Peschel C, Quirt I, Clark JI, Wolchok JD, Weber JS, Tian J, Yellin MJ, Nichol GM, Hoos A, Urba WJ (2010) Improved survival with ipilimumab in patients with metastatic melanoma. N Eng J Med 363:711–723. doi:10.1056/NEJMoa1003466
8. Weber JS, Amin A, Minor D, Seigel J, Berman D, O'Day SJ (2011) Safety asnd clinical activity of ipilimumab in melanoma patients with brain metastases: retrospective analysis of data from a phase 2 trial. Melanoma Res 21:530–534. doi:10.1097/CMR.0b013e32834d3d88
9. Rosenberg S (2011) Cell-transfer immunotherapy for metastatic solid cancer—what clinicians need to know. Nat Rev Clin Oncol 8:577–585. doi:10.1038/nrclinonc.2011.116
10. Sharma P, Wagner K, Wolchok JD, Allison JP (2011) Novel cancer immunotherapy agents with survival benefit: recent successes and next steps. Nat Rev Cancer 11:805–812. doi:10.1038/nrc3153
11. Blank C, Hooijkaas AI, Haanen JB, Schumacher TN (2011) Combination of targeted therapy and immunotherapy in melanoma. Cancer Immunol Immunother 60:1359–1371. doi:10.1007/s00262-011-1079-2
12. Fidler IJ (1973) Selection of successive tumor lines for metastasis. Nat New Biol 242:148–149
13. Smilowitz HM, Weissenberger J, Weis J, Brown JD, O'Neill RJ, Laissue JA (2007) Orthotopic transplantation of v-src expressing glioma cell lines into immunocompetent mice: establishment of a new transplantable in vivo model for malignant gliomas. J. Neurosurg 106:652–659
14. Lowenthal JW, Corthésy P, Tougne C, Lees R, MacDonald HR, Nabholz M (1985) High and low affinity IL2 receptors: analysis by IL2 dissociation rate and reactivity with monoclonal anti-receptor antibody PC61. J Immunol 135:3988–3994
15. Setiady YY, Coccia JA, Park PU (2010) In vivo depletion of CD4+FoxP3+ Treg cells by the PC61 anti-CD25 monoclonal antibody is mediated by the FcgammaRIII+ phagocytes. Eur J Immunol 40:780–786. doi:10.1002/eji.200939613
16. Dranoff G, Jaffee E, Lazenby A, Golumbek P, Levitsky H, Brose K, Jackson V, Hamada H, Pardoll D, Mulligan RC (1993) Vaccination with irradiated tumor cells engineered to secrete murine granulocyte-macrophage colony-stimulating factor stimulates potent, specific and long-lasting anti-tumor immunity. Proc Natl Acad Sci USA 90:3539–3543
17. Cranmer LD, Trevor KT, Bandlamuri S, Hersh EM (2005) Rodent models of brain metastases in melanoma. Melanoma Res 15:325–356
18. Weiss E-M, Wunderlich R, Ebel N, Rubner Y, Schlücker E, Meyer-Pittroff R, Ott OJ, Fietkau R, Gaipl US, Frey B (2012) Selected anti-tumor vaccines merit a place in multimodal tumor therapies. Front Oncol 2:132. doi:10.3389/fonc.2012.00132
19. Dranoff G (2012) Experimental mouse tumour models: what can be learnt about human cancer immunology? Nat Rev Immunol 12:61–66. doi:10.1038/nri3129
20. Fox BA, Schendel DJ, Butterfield LH, Aamdal S, Allison JP, Ascierto PA, Atkins MB, Bartunkova J, Bergmann L, Berinstein N, Bonorino CC, Borden E, Bramson JL, Britten CM, Cao X, Carson WE, Chang AE, Characiejus D, Choudhury AR, Coukos G, de Gruijl T, Dillman RO, Dolstra H, Dranoff G, Durrant LG, Finke JH, Galon J, Gollob JA, Gouttefangeas C, Grizzi F, Guida M, Hakansson L, Hege K, Herberman RB, Hodi FS, Hoos A, Huber C, Hwu P, Imai K, Jaffee EM, Janetzki S, June CH, Kalinski P, Kaufman HL, Kawakami K, Kawakami Y, Keilholtz U, Khleif SN, Kiessling R, Kotlan B, Kroemer G, Lapointe R, Levitsky HI, Lotze MT, Maccalli C, Maio M, Marschner JP, Mastrangelo MJ, Masucci G, Melero I, Nelief C, Murphy WJ, Nelson B, Nicolini A, Nishimura MI, Odunsi K, Ohashi PS, O'Donnell-Tormey J, Old LJ, Ottensmeier C, Papamichail M, Parmiani G, Pawelec G, Proietti E, Qin S, Rees R, Ribas A, Ridolfi R, Ritter G, Rivoltini L, Romero PJ, Salem ML, Scheper RJ, Seliger B, Sharma P, Shiku H, Singh-Jasuja H, Song W, Straten PT, Tahara H, Tian Z, van Der Burg SH, von Hoegen P, Wang E, Welters MJ, Winter H, Withington T, Wolchok JD, Xiao W, Zitvogel L, Zwierzina H, Marincola FM, Gajewski TF, Wigginton JM, Disis ML (2011) Defining the critical hurdles in cancer immunotherapy. J Transl Med 9:214. doi:10.1186/1479-5876-9-214
21. Demaria S, Bhardwaj N, McBride WH, Formenti SC (2005) Combining radiotherapy and immunotherapy: a revived partnership. Int J Rad Oncol Biol Phys 63:655–666. doi:10.1016/j.ijrobp.2005.06.032
22. Smilowitz HM, Micca PL, Nawrocky MM, Slatkin DN, Tu W, Coderre JA (2000) The combination of boron neutron-capture therapy and immunoprophylaxis for advanced intracerebral gliosarcomas in rats. J Neuro-Oncol 46:231–240
23. Smilowitz HM, Coderre JA, Nawrocky MM, Tu W, Pinkerton A, Jahng GH, Gebbers N, Slatkin DN (2002) The combination of X-ray-mediated radiosurgery and gene-mediated immunoprophylaxis for an advanced intracerebral gliosarcoma in rats. J. Neuro-Oncol 57:9–18
24. Formenti SC, Demaria S (2013) Combining radiotherapy and cancer immunotherapy: a paradigm shift. JNCI 105:256–265. doi:10.1093/jnci/djs629
25. Wheeler CJ, Black KL (2009) DCVax-Brain and DC vaccines in the treatment of GBM. Expert Opin Invest Drugs 18:509–519. doi:10.1517/13543780902841951
26. Prins RM, Soto H, Konkankit V, Odesa SK, Eskin A, Yong WH, Nelson SF, Liau LM (2011) Gene expression profile correlates with T-cell infiltration and relative survival in glioblastoma patients vaccinated with dendritic cell immunotherapy. Clin Cancer Res 17:1603–1615. doi:10.1158/1078-0432.CCR-10-2563

27. Gibney GT, Forsyth PA, Sondak VK (2012) Melanoma in the brain: biology and therapeutic options. Melanoma Res 22:177–183. doi:10.1097/CMR.0b013e328352dbef
28. Onizuka S, Tawara I, Shimizu J, Sakaguchi S, Fujita T, Nakayama E (1999) Tumor rejection by in vivo administration of anti-CD25 (Interleukin-2 Receptor α) monoclonal antibody. Cancer Res 59:3128–3133
29. Shimizu J, Yamazaki S, Sakaguchi S (1999) Induction of tumor immunity by removing CD25+CD4+ T cells: a common basis between tumor immunity and autoimmunity. J Immunol 163: 5211–5218
30. Piccirillo CA, Shevach EM (2001) Cutting edge: control of CD8+ T cell activation by CD4+CD25+ immunoregulatory cells. J Immunol 167:1137–1140
31. Tanaka H, Tanaka J, Kjaergaardf J, Shu S (2002) Depletion of CD4+CD25+ regulatory cells augments the generation of specific immune T cells in tumor draining lymph nodes. J Immunother 25:207–217. doi:10.1097/01.CJI0000015083.20350.82
32. Maes W, Rosas GG, Verbinnen B (2009) DC vaccination with anti-CD25 treatment leads to long-term immunity against experimental glioma. Neuro Oncol 11:529–542. doi:10.1215/15228517-2009-004
33. Grauer IM, Sutmuller RP, van Maren W, Jacobs JF, Bennink E, Toonen LW, Nierkens S, Adema GJ (2008) Elimination of regulatory T cells is essential for an effective vaccination with tumor lysate-pulsed dendritic cells in a murine glioma model. Int J Cancer 122:1794–1802. doi:10.1002/ijc.23284
34. Van de Laar L, Coffer PJ, Woltman AM (2012) Regulation of dendritic cell development by GM-CSF: molecular control and implications for immune homeostasis and therapy. Blood 119:3383–3393. doi:10.1182/blood-2011-11-370130
35. Rice JC, Bucy RP (1995) Differences in the degree of depletion, rate of recovery, and their preferential elimination of naive CD4+T cells by anti-CD4 monoclonal antibody (GK1.5) in young and aged mice. J Immunol 154:6644–6654
36. Zou T, Satake A, Ojha P, Kambayashi T (2011) Cellular therapies supplement: the role of granulocyte macrophage colony stimulating factor and dendritic cells in regulatory T-cell homeostasis and expansion. Transfusion 51:160S–168S. doi:10.1111/j.1537-2995.2011.03379.x
37. Jacobs JF, Nierkens S, Figdor CG, deVries IJ, Aderma GJ (2012) Regulatory T cells in melanoma: the final hurdle towards effective immunotherapy? Lancet Oncol 13:e32–e42. doi:10.1016/S1470-2045(11)70155-3
38. Whiteside TL, Schuler P, Schilling B (2012) Induced and natural regulatory T cells in human cancer. Expert Opin Biol Ther 12:1383–1397. doi:10.1517/14712598.2012.707184
39. Lutsiak ME, Semnani RT, De Pascalis R, Kashmiri SV, Schlom J, Sabzevari H (2005) Inhibition of CD4+25+ T regulatory cell function implicated in enhanced immune response by low-dose cyclophosphamide. Blood 105:2862–2868. doi:10.1182/blood-2004-06-2410
40. Peggs KS, Quezada SA, Chambers CA, Korman AJ, Allison JP (2009) Blockade of CTLA-4 on both effector and regulatory T cell compartments contributes to the antitumor activity of anti-CTLA-4 antibodies. J Exp Med 206:1717–1725. doi:10.1084/jem.20082492